6D.4

# VARIABILITY OF ATMOSPHERIC MOISTURE DURING THE BOREAL SPRING IN WEST AFRICA

Roberto J. Mera[1,*], Arlene Laing[2], and Fredrick H.M. Semazzi[1]

[1]North Carolina State University, Raleigh, North Carolina
[2]National Center for Atmospheric Research, Boulder, Colorado

## 1. INTRODUCTION

### 1.1 *Motivation*

Weather and climate in the African Sahel are dominated by two major wind systems, the southwesterly West African Monsoon (WAM) and the northeasterly (Harmattan) trade winds. As the primary driver for precipitation, the WAM is a vital component of the socio-economic environment of the region. In addition to the agricultural benefit of the rains, the public health sector is affected due to the relationship between the onset of monsoon moisture and end of meningitis outbreaks (Molesworth et al., 2003). Knowledge and prediction of moisture distribution during the boreal spring is vital to the mitigation of meningitis by providing guidance for vaccine dissemination. Yet the boreal spring has received little attention in the literature; in contrast the summer monsoon has been the subject of numerous studies (Reed et al. 1977, Sultan and Janicot 2003, Kiladis et al. 2006) and field campaigns such as the Global Atmospheric Research Program (GARP) Atlantic Tropical Experiment (GATE, Kuettner and Parker 1976), and the African Monsoon Disciplinary Analysis (AMMA, Redelsperger et al., 2006).

Much of what is known about the climate/environmental factors relevant to meningitis has been based on annual and seasonal data. Meningitis epidemics tend to occur in sectors of West Africa that exhibit particular environmental characteristics. Ongoing research indicates that along with moisture (relative and absolute humidity), incidence of the disease can also be affected by land-cover type (e.g. arid, semi-arid, tropical forest), dust loading in the atmosphere and surface temperature. The most robust and actionable climate/meningitis relationship arises from the strong correlation between the start of the rainy season and the abrupt decline in the transmission of the disease (Molesworth et al., 2003). The critical variables associated with meningitis outbreaks are very low humidity and dusty conditions (Besancenot et al 1997); while cessation occurs with the onset of rains (Molesworth et al. 2003). Sultan et al. (2005) found a strong correlation between the timing of the epidemic onset in Mali and the winter wind maximum but could not differentiate low and high incidence years. Yaka et al. (2008) found that variations in surface winds can explain 25% of the year-to-year differences in meningitis outbreaks in Niger. Thomson et al. (2006) found that anomalies in annual meningitis incidence at the district level in Burkina Faso, Niger, and Mali were related to monthly climate anomalies. Although questions remain about the initiation of outbreaks, a clear pattern has emerged in the cessation of the disease, brought about by the advent of moist conditions.

While there is no consensus on which measure of humidity and other environmental variables correlate best with meningitis incidence, a few studies provide some guidance. For example, Greenwood et al. (1979) used absolute humidity and mean maximum temperature while Thomson et al. (2006) examined rainfall, satellite-derived dust loading, and vegetation indices. Besancenot et al. (1997) identified three meteorological conditions associated with the Harmattan regime and meningitis epidemics: minimal mean temperature of no more than 20 °C, a mean relative humidity of no more than 40%, and the presence of at least three days of dust haze. The present study uses the 40% surface relative humidity (RH) as a threshold for alleviation of epidemic conditions.

Providing information on the predictability and outlook for meteorological conditions that have an appreciable correlation with the cessation of disease epidemics will guide allocation of scarce vaccines to regions likely to remain dry. Our study complements ongoing research at the University Corporation for Atmospheric Research (UCAR) by evaluating the skill of the Weather Research and Forecasting Model (WRF) at spatial resolutions (district level) and timescales that are relevant to meningitis management in the region.

### 1.2 *The pre-onset of the monsoon and the Intertropical Front (ITF)*

Meteorological signals prior to the start of the WAM are weak at a regional scale because rainfall initiation over the Sudano−Sahelian zone is seldom abrupt in nature and it is usually preceded by a succession of isolated precipitation systems of uncertain intensity interspersed with dry periods of varying duration (Omotosho et al., 2000; Ati et al. 2002). In order to understand the persistence, strength and variability of the early season WAM rains, it is important to analyze the behavior of the ITF. As introduced by Hamilton and Archbold (1954), Eldridge (1957), Hare (1977), and later expanded on by Sultan and Janicot (2003) and Lélé and Lamb (2009), the ITF is an integral part of the buildup and retreat of the WAM. Lélé and

*Corresponding author address: Roberto J Mera, North Carolina State University, Dept. of Marine, Earth and Atmospheric Sciences, Raleigh, NC 27695; e-mail: rjmera@ncsu.edu

Lamb (2009) postulated that the location of the ITF in April could be used as a predictor for the advancement of the leading edge of the southwest monsoon flow during the May-June period. Sultan and Janicot (2003) diagnosed this critical feature as one where the first isolated precipitation systems occur ahead of the WAM.

The definition of the ITF, in terms of the variables used to derive its location and behavior, is calculated differently in recent studies. Lélé and Lamb (2009) used daily temperature, humidity, and rainfall data at 10-day (dekad) resolution to calculate concurrent monthly ITF-rainfall relations. In Sultan and Janicot (2003), the ITF is defined by the 925 hPa zero isoline of the zonal wind (where the westerly monsoon winds begin). Another marker of the ITF is the 15°C dewpoint temperature (Pospichal et al. 2006). This paper uses mostly the Sultan and Janicot's (2003) definition of the ITF since they also identify short rains at the northern boundary as an essential feature in the progression of the WAM. The Intertropical Convergence Zone (ITCZ) is most often identified by the band of precipitation to the south of the ITF.

The ITF, which is also defined as the Intertropical Discontinuity (ITD), is strongly affected by the variability of the Saharan Heat Low (SHL). The SHL is an extension of the equatorial trough and the pressure gradient between the SHL and the subtropical high controls the strength of the Harmattan. Recent studies suggest that the monsoon onset is partly controlled by the SHL dynamics (Sultan and Janicot, 2003; Drobinski et al., 2005; Ramel et al., 2006; Sijikumar et al., 2006).

Unusual dry season rain events are a potentially-predictable source of precipitation during the dry season that could affect the progression of the ITF and WAM. In Knippertz and Fink (2008), their case study of a January precipitation event in West Africa associated with a mid-latitude disturbance in 2004 occurs in a year that saw the ITF arrive at 15°N 23 days in advance of the climatological arrival of this dynamical feature. The connection between the arrival of ITF (and the associated short convective systems) and feedbacks from short term events during the dry season can have important impacts on the initiation and evolution of convection during the dry-to-rainy season transition.

Moisture and precipitation over West Africa is associated with synoptic disturbances including African easterly waves, the dominant synoptic system during the boreal summer (Reed et al. 1977; Diedhiou et al. 1999; Kiladis et al. 2006; Mekonnen et al. 2006). Convection is also modulated by intraseasonal circulations such as equatorial waves and the Madden-Julian Oscillation (MJO), a major source of precipitation and moisture variability in the tropics. The relationship between synoptic dynamical disturbances and the larger intraseasonal circulations is an area of active study. Mekonnen et al. (2008) found that equatorial Kelvin waves enhance easterly waves during the boreal summer. Mournier et al (2007) described a case where a Kelvin wave was critical to the summer monsoon onset. Since Kelvin waves are active during the boreal spring, it is imperative to understand how they relate to convection and moisture variability over West Africa

The aim of this study is to describe the variability and prediction of surface moisture in West Africa using simulations, global model analyses, satellite observations, and local station observations. We will diagnose some fundamental dynamical characteristics of the boreal spring in West Africa under certain critical synoptic and climatological states. From this we will infer the meteorological factors pertinent to meningitis mitigation at intraseasonal timescales.

## 2. DATA AND METHODS

### 2.1 *Data, Domain, and Period of Study*

The study domain is centered on West Africa and large enough to encompass cross-equatorial and midlatitude influences that may affect regional moisture variability (Fig. 1). The simulation periods are January to August of 2000 to 2009. Synoptic climatologies for April and May of each year were developed using the National Centers for Environmental Prediction (NCEP)/ National Center for Atmospheric Research (NCAR) Reanalysis or NNRP (Kalnay et al., 1996). We chose 2006 because of the significant amount of station observations during AMMA (Redelsperger et al., 2006) and we use the station in Niamey, Niger (13°27'N, 02°06'E) to analyze model results at a specific location. .

Standard meteorological surface observations are used to diagnose the position of the ITF, the shift to the monsoon moisture regime, and for validation of the model simulations. Daily mean outgoing longwave radiation (OLR) data with a spatial resolution of 2.5° (Liebmann and Smith 1996) are used as a proxy for convective activity. Rainfall observations are the Tropical Rainfall Measurement Mission (TRMM) Multi-satellite Precipitation Analysis, a gauge calibrated 3-hourly dataset with a 0.25° x 0.25° grid (Huffman et al. 2007). Mixing ratio at 925 and 850 hPa from the Atmospheric Infrared Sounder (AIRS) instrument (Aumann et al. 2003) are used to validate simulated lower-tropospheric moisture. A parcel back-trajectory analysis utilizing the horizontal and vertical wind components, as well as RH (%) from the NNRP, is employed to compute the sources of air parcels for the points bounded by 10°W-10°E and 10°N-15°N for the years 2000-2008. The 925 hPa level was chosen as the endpoint surface to circumvent noise generated in the reanalysis below 925 hPa, where parcels can intercept the ground.

Reduced dimension analysis (Hovmoller diagrams) of anomalies of OLR, precipitable water, and rainfall are used to identify westward and eastward propagating modes of tropical convection. Space-time filtering of the OLR is used to isolate the tropical modes of interest using the techniques of Wheeler and Kiladis (1999).

### 2.2 *Model Configuration and Simulations*

A dual-nested domain simulation is performed using a mass-coordinate version (3.0) of the Advanced

Research WRF (ARW) modeling system (Skamarock et al. 2008). This study uses a 90-km grid for the outer domain, 30 km for the inner domain, and 27 vertical levels. The physics schemes utilized include the WSM3-class simple ice scheme (microphysical), Kain-Fritsch (cumulus physics), Monin-Obukhov (surface layer), Yonsei University (YSU) (planetary boundary layer), Noah Land Surface model, and CAM radiation. The model has been adapted for regional climate and real time forecast with spin-ups for seasonal simulations that start during the boreal winter. Specific years in the calibration analysis are 2006 and 2009. The model configuration was chosen for long simulations at optimal computational rates while retaining the best physics schemes for that region. Choices were also guided by previous studies, such as Flaounas et al (2009), who found that the Kain-Fritsh scheme was appropriate for West Africa. The initial and lateral boundary conditions are obtained from NCEP Global Forecast System (GFS) Final Analyses (FNL) which has 1˚ x 1˚ horizontal grid, and is available at six-hourly synoptic times, and daily sea surface temperatures (SSTs) derived from the FNL skin temperature.

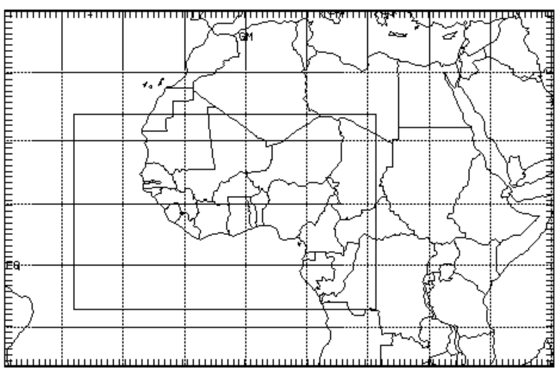

Figure 1. Inner and outer domain for WRF simulations

During January to June 2009, numerous experimental forecasts (ensembles of 8 members) were used to diagnose real-time humidity changes and precipitation. At the end of the boreal spring, we performed a season-long simulation and compared it against weekly attack rates reports, in-situ observations and the global reanalysis. Seasonal simulations were also performed for 2000 to 2008 but most of the discussion will focus on 2009.

## 3. CONCEPTUAL MODEL AND SYNOPTIC CLIMATOLOGIES

### 3.1 *General Features*

Before delving into the detailed study of moisture variability, it is imperative to understand the major features and modulators of West Africa circulation during the boreal spring. The boreal spring is marked by the northward advancement of the monsoon. During this period, the WAM reaches its pre-onset stage and is followed by the onset (late June) and the summer monsoon from July through September. The pre-onset of the monsoon is closely linked with the position of the ITF in West Africa (Sultan and Janicot, 2003; Lélé and Lamb, 2010), and the various interactions that govern its state and the associated atmospheric and ocean patterns.

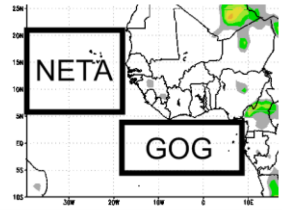


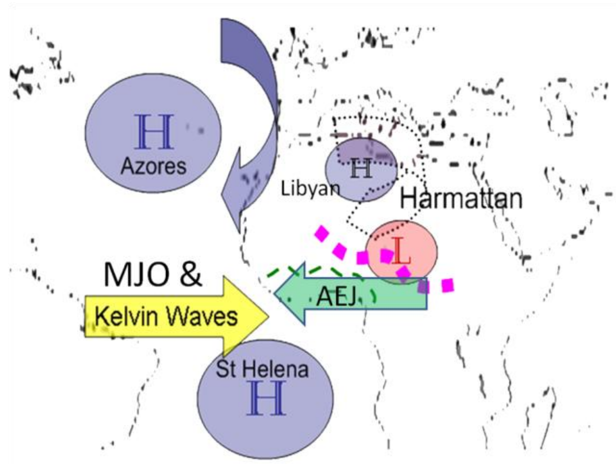


Figure 2. Main attributes of the general circulation patterns during the boreal spring..

During the summer, the ITF (green dashed curve) is as far as 20°N and the precipitation maximum is at about 10°N in the southern fringes of the Sahel. During the boreal spring, the bulk of the precipitation is limited to the coast along the Gulf of Guinea at 5°N. Additionally, most of the region is governed by dry, dusty Harmattan winds emanating from the Saharan desert. In Fig. 2 we present a conceptual model of WAM features during the boreal spring. The blue curved arrows represent airflow around the Azores and Libyan anticyclones. The airflow around the Libyan anticyclone fuels the Harmattan northeasterlies, aided by the pressure gradient created with the West Africa Heat Low (WAHL) and the ITF (pink, dotted). The dominant large-scale circulation features are the Azores and the Libyan anticyclones in the north and the St. Helena anticyclone in the south (Adedokun, 1978; Dohneur, 1970).

The large-scale components are complemented by smaller but integral dynamical features and surface conditions. One such feature is the African Easterly Jet (AEJ, green arrow), which varies from a position of about 3°N and 700 hPa in mid March to about 9°N and 600 hPa in mid June (Afiesiamama, 2007). Equally essential to the overall mechanics of the monsoon are the waters of the Gulf of Guinea (GOG) and the North East Tropical Atlantic (NETA) (Fig. 2). Indeed, much of the interannual and decadal variability of WAM precipitation are associated with anomalous SSTs in these two regions (Vizy and Cook, 2001; Xie and

Carton, 2004; Hagos and Cook, 2007). Other relevant surface features include the meridional gradient of land cover, northward from the forests close to the GOG to the grasslands of the Sahel, and the Saharan desert.

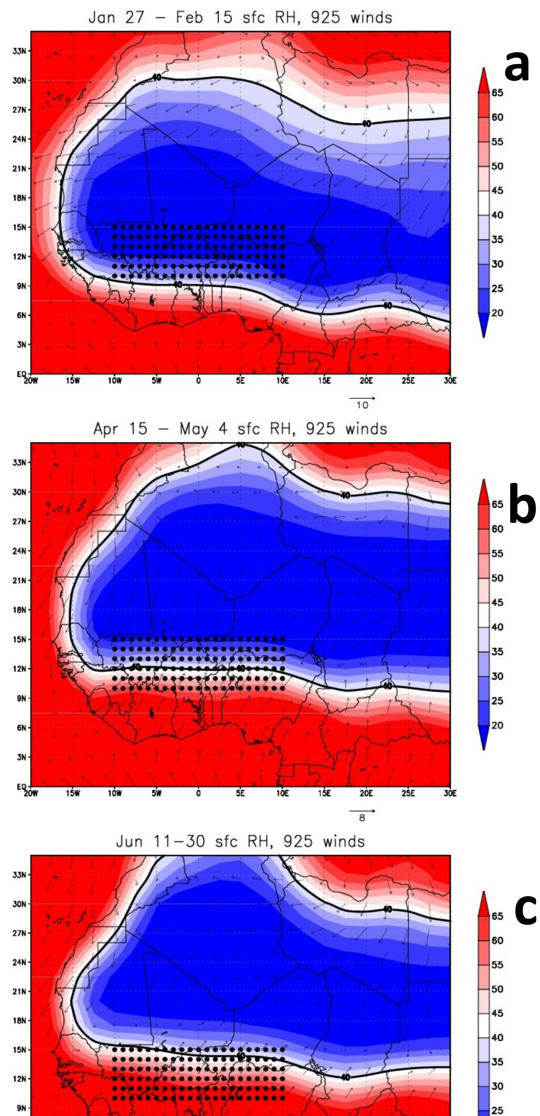


Figure 3. end point matrix, RH (%) during (a) Jan 27 – Feb 15, (b) Apr 16 – May 4, (c) Jun 11 -30. (2000-2008 averages)

Teleconnections and interactions with mid-latitude systems and the general circulation also determine the state of the WAM during the spring. For instance, it has been shown that mid-latitude systems can extend their influence deep into the tropics, causing anomalous precipitation (Knippertz and Fink 2008, 2009).

Table 1. Date 40% RH threshold is crossed at each latitude inside the study area.

| Latitude | Date RH Threshold is crossed |
|---|---|
| 10°N | 24-Mar |
| 11°N | 18-Apr |
| 12°N | 29-Apr |
| 13°N | 5-Jun |
| 14°N | 21-Jun |
| 15°N | 29-Jun |

### 3.2 *Migration of the ITF and Parcel Trajectory Analysis*

The relative humidity from the NNRP for the period 2000 to 2008 is used to diagnose the climatology of the monsoon moisture. The threshold (40%) is used as a proxy for the shift from Harmattan conditions to the WAM regime (Besancenot et al. 1997). The mean arrival time of the 40% surface RH varies meridionally (Table 1). As defined, the changes coincide with the general position of the ITF, which remains at a quasi-stationary position between 10N and 12N from late March through mid May. The latitude of the ITF is most variable during mid-April to mid-June. It typically reaches 15N near the end of June, which is also the start of the West African monsoon (Sultan and Janicot, 2003).

Because the rate of advance varies, monthly analyses are inadequate. Instead, the moisture regimes are classified into three 19-day periods: before (P1, January 27 − February 15), during (P2, April 15 − May 4), and after (P3, June 11 − 30) the passage of the ITF through the region. As seen in Fig. 3, the focus region is completely immersed in the dry Saharan air during P1 (3a), partially within the moist environment of the WAM during P2 (3b), and almost entirely outside of the dry Saharan air in P3 (3c). For each period, the following winds prevailed: strong northeasterlies for P1, a mix of northerly and northeasterlies for points north of the 40% line and WAM southwesterlies to the south for P2, and southwesterlies for P3 even for points that remain below 40%. The source points vary in spatial scale both in their horizontal and vertical components. Vertically, source points during P1 are located in the mid to upper levels of the atmosphere (750-600 hPa), on average, with a wide spectrum of vertical source points during P2 (900 to 650 hPa), and strictly lower-level points during P3 (<800 hPa)..

Further analysis of the source points for each of the periods shows the proportion of air parcels from each of the geographical areas (Fig. 4) adjacent to and including the study region. During P2 (Fig. 3b), the majority of source points (44%) still have a source region in NW Sahara (Fig. 4). The second highest density (20%) occurs over the South Atlantic region, with 14% for the Gulf of Guinea (GOG) and 8% within our box (Sahel). Smaller percentages represent areas like the GOG coast, North-east Tropical Atlantic (NETA) and NE Sahara.

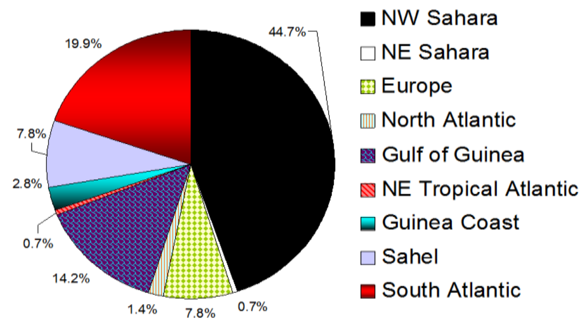


Figure 4. Distribution of air mass source regions during the mid-spring (P2 in Fig. 3).

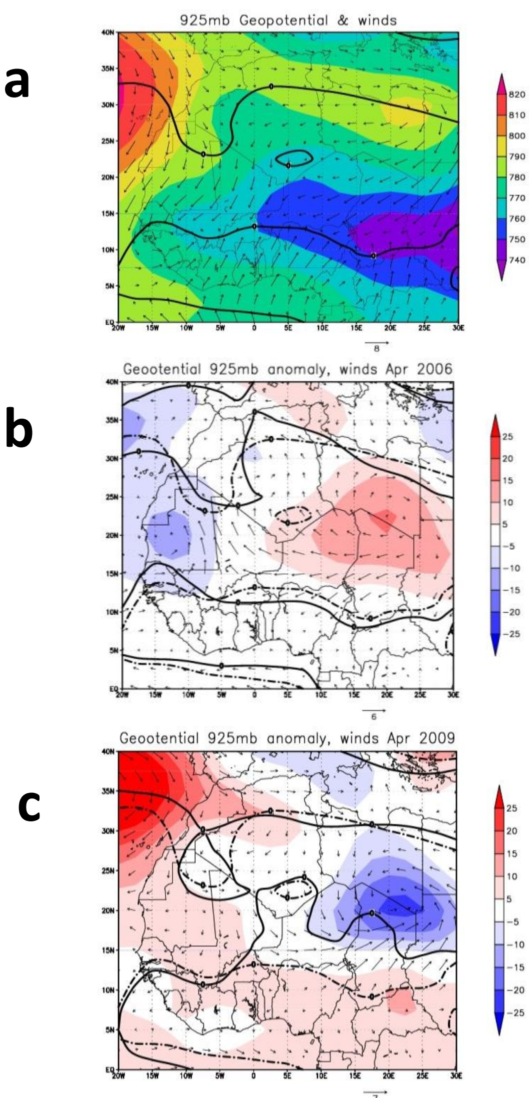


Figure 5. Geopotential height and winds at 925 hPa for April (a) 2000-2009 climatology, (b) 2009, and (c) 2006. In (b) and (c), the position of ITF is solid and dash-dotted for the 2000-2009 climatology.

### *3.3 Synoptic Climatologies for 2006 and 2009*

During the 2009 boreal spring, bi-weekly real-time simulations were used to diagnose the model's capabilities. This provided a rich dataset to test the model's skill against *in-situ* and remotely-sensed observations. Additionally, district-level meninigitis epidemic data were also available for the country of Nigeria. We compare the 2009 season with the 2006 season, a period with rich amounts of information generated by the AMMA campaign. The two years also served as a study in contrast; exemplified by the synoptic conditions during the month of April (Fig. 5). The position of the ITF is contoured for 2006 and 2009 (solid) and climatology (dash-dot).

The 925 hPa winds and geopotential height fields (Fig. 5) derived from the NNRP are used as a proxy for the location of the WAHL (Lavaysse, 2009), the climatological equatorial trough and the associated flow. During 2006, anomalous anticyclonic circulation over the Sahara, in association with the WAHL and Libyan Anticyclone pressure gradient, caused anomalous, strong Harmattan flow that pushed the moisture front south of its climatological position (Fig. 5b). In comparison, 2009 (Fig. 5c) had the opposite: a strong cyclonic anomaly was present north of the climatological WAHL, with increased monsoon flow that penetrated well into the Sahel. The contours show the position of the ITF for 2006 and 2009 (solid, 5b, 5c) and the climatology (dotted). Note the more southerly location of the ITF in 2006 compared to 2009.

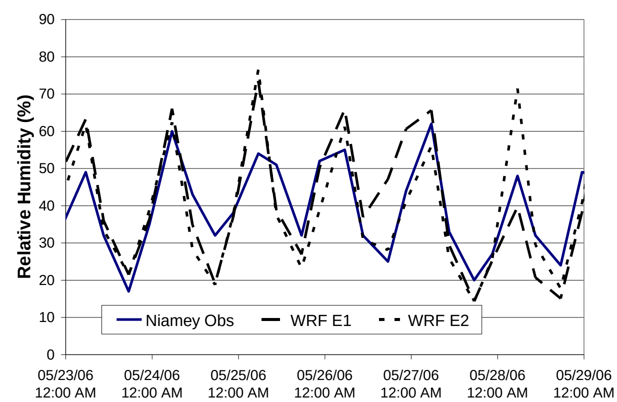


Figure 6. Diurnal variability of RH (%) as given by station data at Niamey (solid blue), and two simulations from the physics parameterization tests, E1 (dashed black) and E2 (dotted black).

## 4. REGIONAL MODEL DIAGNOSTICS

Validation of the regional model, the ARW, is a necessary part of assessing its usefulness as a tool for forecasting moisture variability in West Africa. The focus is primarily on general statistics such as spatial distribution of moisture, the diurnal cycle, and temporal variability of the 40% RH threshold. A few examples are presented.

**4.1 *Simulations in 2006***

Given the importance of diurnal variability to monsoon dynamics (Parker et al 2005), the ITF advances during the nighttime, we examined the model's skill at this scale (Figure 6). From the physics parameterization sensitivity tests for 2006, two of the model schemes were able to capture the diurnal cycle fairly well (Fig. 6). The 2006 validation tests showed a negative bias in surface temperature for a group of simulations that included "Thermal Diffusion" as a land surface model option. This cold bias (not shown) caused higher humidity throughout the region, rendering it unusable for the prediction of moisture that is necessary for meningitis mitigation.

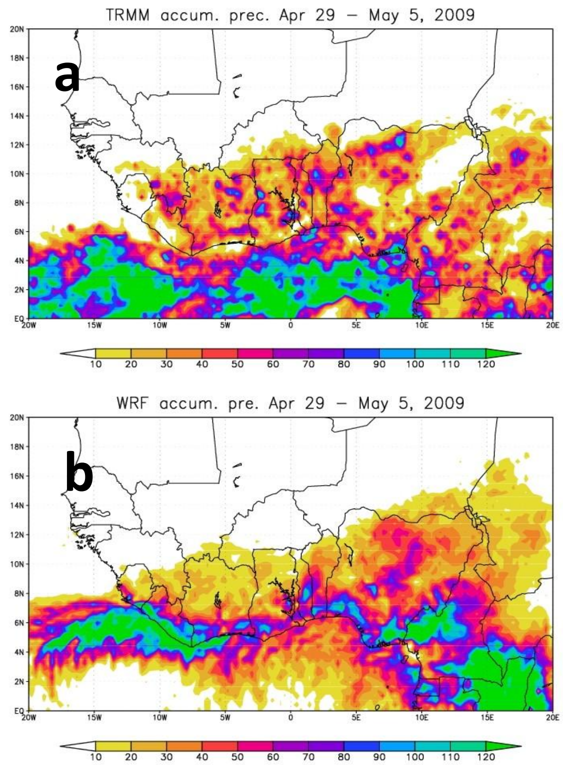


Figure 7. TRMM-derived (a) and model-simulated total (b) accumulated rainfall for April 29 – May 5, 2009.

**4.2 *Simulations in 2009***

The 2009 boreal spring provided a good test bed for gauging the model's capability to simulate atmospheric moisture and precipitation. Here, we compared the model results against satellite observations from the 3-hrly TRMM MPA (Huffman et al. 2007) and mixing ratio at 925 and 850 hPa from the AIRS instrument. Accumulated precipitation for the week of 29 April – 5 May 2009 is presented in Fig. 7. The model captures the overall spatial structure of precipitation patterns over the region as portrayed by TRMM, but this positive result is limited to the continent. The figure also shows that the model is unable to capture the ITCZ over the GOG.

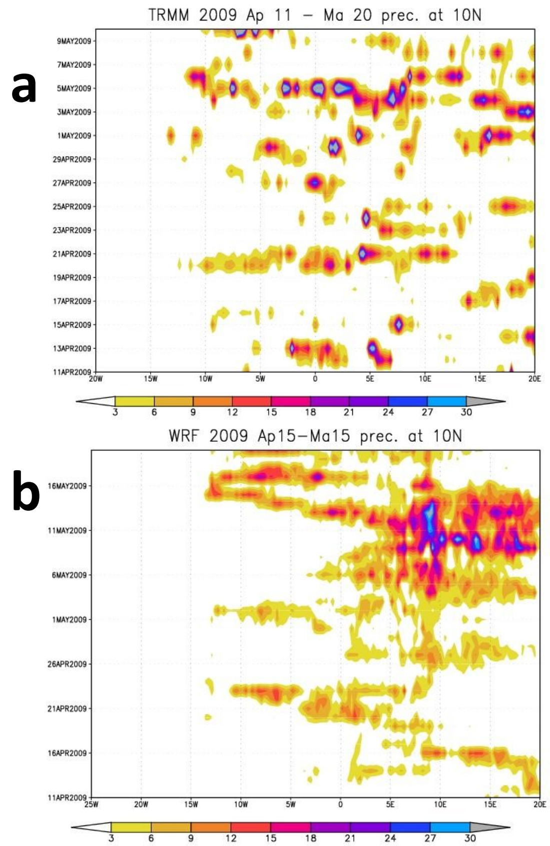


Figure 8. Hovmoller diagram of TRMM-derived (a) and WRF simulation of accumulated precipitation at 10°N latitude from 20°W to 20°E during April and May of 2009.

The model's ability to capture precipitation over the land is significant because it helps to diagnose the dynamical features associated with shifts in the moisture over the vulnerable Sahel. A Hovmoller plot of precipitation averaged for points along 10°N is shown in Fig. 8. The model is able to capture the overall structure of westward-propagating systems and actually provides more information about the progression of these features through the region. The limitations of satellite-estimated precipitation must be considered when comparing it against the model precipitation, as it is possible that some of the rainfall may not be observed by the satellite due to its orbit or other documented biases (Wolf et al. 2008).

Given the main objectives of this study, it is vital to analyze the model's ability to predict the three-dimensional distribution of moisture. In Fig. 9, the 925 hPa mixing ratio observed by the AIRS is compared against the same field from WRF for 6-12 May 2009. The observations from the satellite occur during 13:30 UTC (also local time in the central study domain). The model outputs data on a 6-hourly basis, so we use the 1200 UTC output, the closest available time . The model captures a diagonal moisture plume that extends from the GOG into northern sectors of the country of Niger (into the Sahara Desert) for the 6-12 May period. There is a dry bias over the western portion of the domain from 5°E to 15°W.

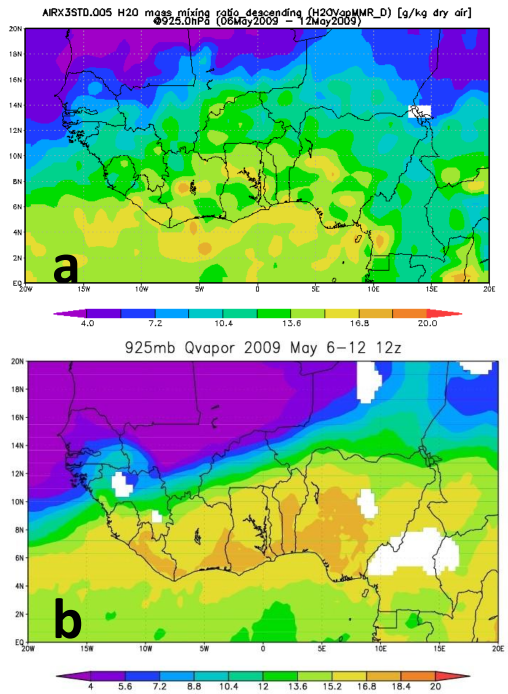


Figure 9. 925 hPa mixing ratio for May 6-12 from AIRS satellite (a), and WRF (b).

The most critical predicted variable for meningitis is surface moisture. Figure 10 presents the area averages of WRF-derived dewpoint temperature over two different cities: Tambacounda (Senegal) and Niamey (Niger). The model time series is closely aligned with the observations, especially the shift in the moisture regime from the variable spring conditions that are characterized by sharp moist events, to the more stable monsoon conditions once the moisture the 15°C dewpoint threshold. It should be noted, however, that although the model produces moisture spikes, some of these are not produced on the observed dates. From the synoptic climatologies (Section 3), we also know that Tambacounda is susceptible to variability in the oceanic circulations from the northwest and southwest. Yet, in terms of correlations, Tambacounda is higher (0.86) than Niamey (0.8) mainly because, although the model has a dry bias, there are fewer instances where moisture spikes are misclassified as dry or moist.

.

## 5. MID-SPRING MOIST EVENTS AND CONVECTIVELLY-COUPLED EQUATORIAL WAVES

During the same period as experimental real-time forecasts in 2009, highly-detailed meningitis data became available for the country of Nigeria. This, coupled with a well-maintained in-situ observation station in the northern city of Kano, facilitated an in depth examination of synoptic and intraseasonal cycles, their effects on moisture variability and their possible role in meningitis trends.

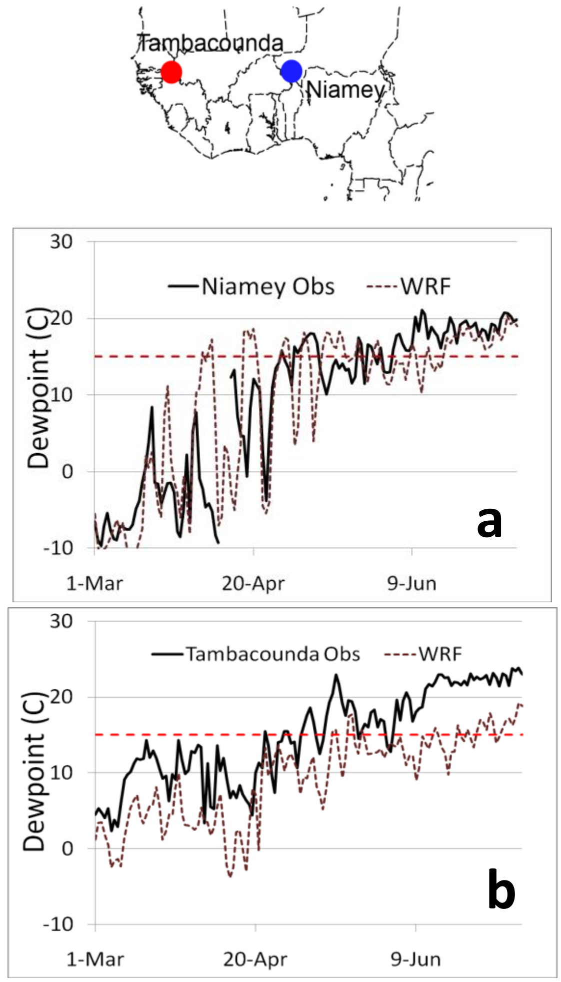


Figure 10. Time series of dewpoint temperature for observed (solid) and WRF-simulated (dotted) for Niamey (a) and Tambacounda (b).

Specifically, we investigate the occurrence of "moisture spikes" in the real-time simulations, which were later confirmed by station observations. These events produced a shift in the moisture regime for the city of Kano. The moisture spikes were later linked to transient westward-propagating features. Figure 11 shows three distinct spikes in the relative humidity field. With each event, the humidity regime was elevated to a new level. Given the evident shift in the moisture, an intriguing question was asked,

What could be causing these moisture surges?

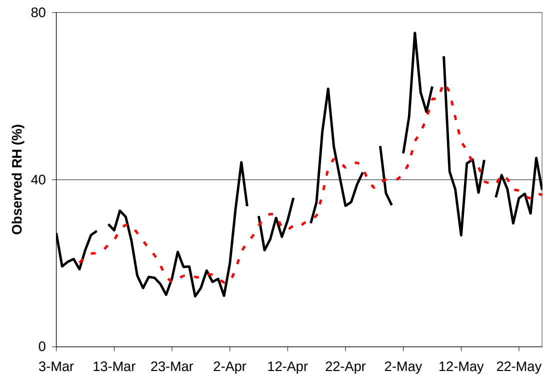


Figure 11. Time series of observed RH (%) for the city of Kano, Nigeria during spring 2009. Red dashed line is the 7-day running mean.

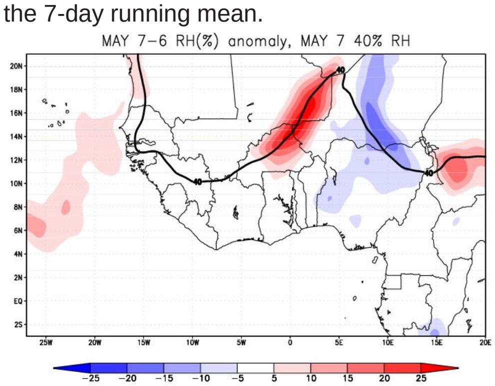


Figure 12. West Africa real-time forecasts for (a) May 7-6 day anomaly for changes in RH (%).

### 5.1 *Westward-propagating systems*

The occurrence of westward-propagating features first became evident with a forecasted event during mid-May (Figure 12). This prompted an analysis of humidity at other stations (including Niamey and Tambacounda in Fig. 10) which elucidated the fact that the event is (i) westward-propagating and (ii) significant enough to shift the moisture regime for all locations.

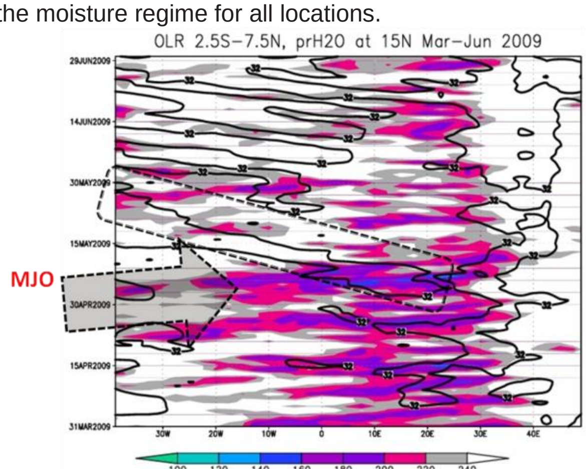


Figure 13. Hovmoller diagram of OLR averaged for 2.5°S to 7.5°N (shaded) and precipitable water at points at 15°N latitude (contour) during the spring of 2009.

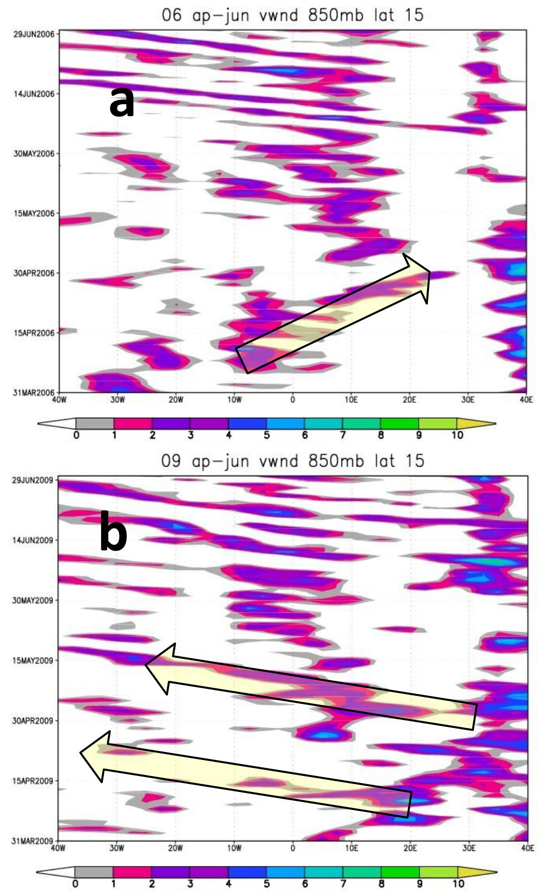


Figure 14. Hovmoller diagram of April-May meridional wind component at 850 hPa for 15°N latitude points during 2006 (a) and 2009 (b).

The OLR field is averaged over 2.5°S – 7.5°N (where most of the activity occurs) and related to reanalysis fields such as precipitable water over the Sahel From the Hovmoller diagram in Figure 13, we note that a weak MJO and an associated Kelvin wave are traversing the region during this part of May 2009. Concurrently, a moist event begins its westward propagation along 15°N from the 20°E longitude. For comparative purposes, Figure 14 shows the unfiltered meridional wind component Hovmoller diagram for 2006 and 2009 from the NNRP reanalysis. Note that more westward-propagating systems are present in 2009 during April and early May in comparison to 2006, where an eastward-propagating feature is visible but little other activity is evident. It should be noted that 2006 had a much drier April and May throughout the domain and the summer monsoon was also delayed (Janicot et al. 2008).

The MJO mentioned above was observed and documented by the NOAA Climate Prediction Center (CPC, [http://www.cpc.noaa.gov/products/precip/CWlink/MJO/ARCHIVE/PDF/mjo_evol-status-fcsts-20090706.pdf](http://www.cpc.noaa.gov/products/precip/CWlink/MJO/ARCHIVE/PDF/mjo_evol-status-fcsts-20090706.pdf)). The Kelvin wave, however, was derived in this study using the Wheeler and Kiladis (1999, hereafter WK99) method. Details of the wavenumber–frequency filtering technique, as well as its merits and implications are described in WK99 and Wheeler et al (2000). The WK99 method has also been successfully applied in other studies based on OLR (e.g., Straub and Kiladis 2002; 2003a; 2003b), and precipitable water data (Roundy and Frank 2004). The WK99 method decomposes a data field into wavenumber–frequency components for eastward- and westward-moving wave types. This allows for the identification of different wave modes in space and time.

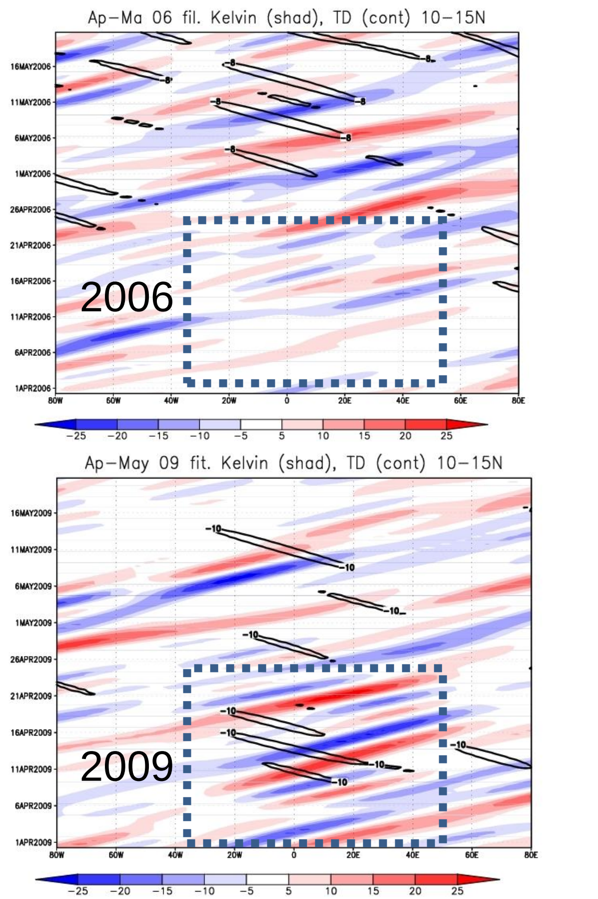


Figure 15. Hovmoller plots for Kelvin filtered OLR averaged for the points 10°N to 15°N for 2006 and 2009. The dotted box highlights the difference in wave activity for both years.

Of particular interest are equatorial Kelvin waves and tropical depression (TD) modes that were prominent during the period of moisture spikes. The latter are westward-propagating features similar to tropical depressions

The Kelvin-filtered and TD-type filtered waves are shown in a Hovmoller plot for the 10°N-15°N averages (Figure 15). Note that 2009 had an active TD field over the domain, further confirmation of the westward features present in the Kano observations (Figure 11). We also see a considerable number of coherent Kelvin waves during this period, suggesting a link between the two features. In contrast, 2006 had limited and weak Kelvin wave activity over the domain (Fig. 15).

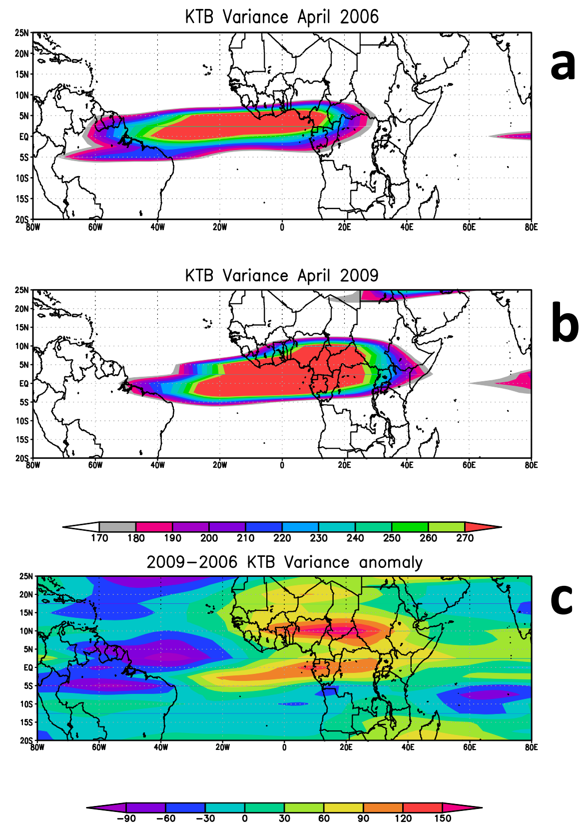


Figure 16. Kelvin-filtered OLR variance for April 2006 (a), 2009 (b) and 2009-2006 anomaly (c).

Further analysis of Kelvin wave activity elucidates the possible influence of these equatorial waves on moisture over the region. Figure 16 shows the variance of the Kelvin-filtered OLR fields over the region. The anomaly (2009-2006) shows significant activity during 2009 over West Africa, especially along the 10°N latitude extending from the Atlantic coast into the Sudan. An overlay of the April 2009-2006 anomaly of Kelvin wave variance on the TD-type variance (Fig. 17) allows for further examination of the possible interaction between these two types of waves: higher Kelvin wave activity for the region bounded by 7.5°N-12.5°N and 0°E-30°E is present at the same time as increased TD-type variance within a sector bounded by 7.5°-15°N and 20°W-15°E.

### 5.3 *Eastward and westward-propagating events in model simulations*

As described earlier, the regional model is being considered as a tool for predicting moisture variability. Given the association of convectively-coupled equatorial waves and westward propagating synoptic systems with dramatic increase in the moisture, it is imperative to test the model's ability to reproduce these systems.

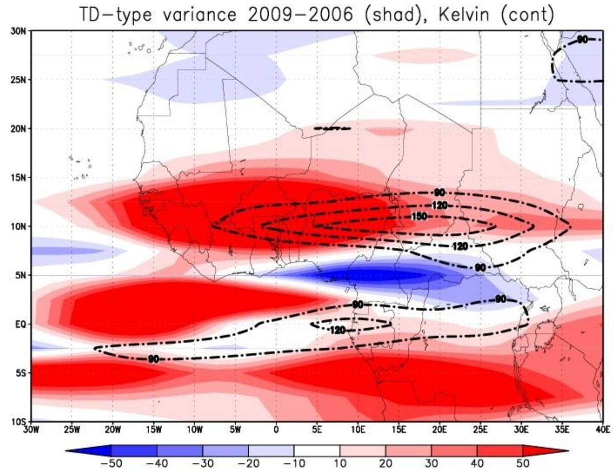


Figure 17. Filtered OLR 2009-2006 anomaly for TD-type (shaded) and Kelvin (contoured).

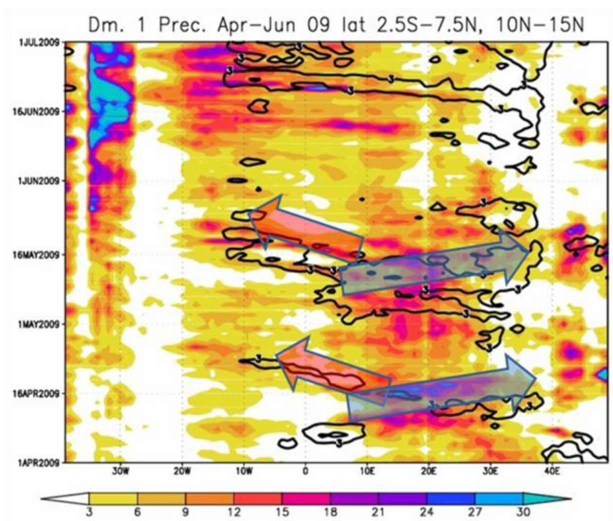


Figure 18. Top: Kelvin-filtered OLR variance anomaly for 2009-2006. Bottom left: Kelvin variance for April 2006. Bottom right: Kelvin variance for 2009.

An analysis of the outer domain allows for the examination of longer-scale and larger-size features, such as MJO or Kelvin waves. From Fig. 8, we note that the inner domain in the model is capable of reproducing westward-propagating features, especially the mid-May event and also two others that occurred in the month of April. The larger-scale MJO and Kelvin features are more clearly visible in the precipitation field for the outer domain (Fig. 18). Similar to Fig. 12, the accumulated precipitation variable is shown for the 2.5°S – 7.5°N latitude band (shaded) in comparison with the same variable at 10°N-15°N (contoured), within the area of interest. In this unfiltered view, the westward-propagating events over the Sahel are superimposed over coherent eastward-propagating features at the lower latitudes. For these particular cases, the presence of a Kelvin wave is followed by a prominent TD-type disturbance that propagates westward with the general flow.

## 6. SUMMARY AND CONCLUDING REMARKS

The present study analyzes the variability of atmospheric moisture during the boreal spring in order to aid mitigation efforts for the climate-sensitive meningitis disease. A conceptual model of the boreal spring over West Africa was presented. We have shown that surface moisture is highly dependent on the position of the ITF and that the ITF varies meridionally and temporally with the seasonal cycle. The timing of the arrival of moist conditions varies on interannual scales and is highly influenced by intraseasonal phenomena such as equatorial Kelvin waves and TD-type disturbances. It was also found that 2009 and 2006 were vastly different in terms of synoptic climatological conditions (anomalous cyclonic WAHL in 2009 compared to anticyclonic circulation in 2006), and Kelvin and TD-type wave activity.

As the 2009 spring season transitioned to the summer monsoon, a season-long simulation using FNL boundary conditions was conducted over the region to assess the relative value of limited-area model's performance in diagnosing meningitis risk relative to the NCEP/NCAR reanalysis.. The end of the meningitis season also provided high resolution information about the disease epidemic, attack rate, and spatiotemporal variance throughout the period (Multi-disease Surveillance Center, 2009).

Data from the district of Kano was used to explore the application of the regional model to meningitis trends with the caveat that trends in the disease can be affected by other factors (Thomson et al. 2006). Figure 19 shows the meningitis attack rate (Number of cases / 100,000 per week, black-white bars) is higher (~20%) during the beginning of the period (late March through early April) when the observed relative humidity (blue) is below 30% over the city of Kano. The attack rate significantly collapses below 8% in mid to late April as the observed relative humidity increases to about 40%, once again suggesting the relationship between moisture and the disease. The season-long WRF simulation (red) is very close to the observed, thus adding significant value to the use of dynamical downscaling. In contrast, NCEP/NCAR reanalysis (green) overestimates moisture well beyond the observed (by about 20%) during the dry period.

This study demonstrates the promise of regional models to provide guidance for some mechanisms that can dramatically shift the moisture and possibly contribute to the mitigation of meningitis in West Africa. Further study is needed to better understand the multi-scale interactions that contribute to the variability of moisture during the boreal spring and to isolate the impact of weather and climate relative to other influences on public health in West Africa,

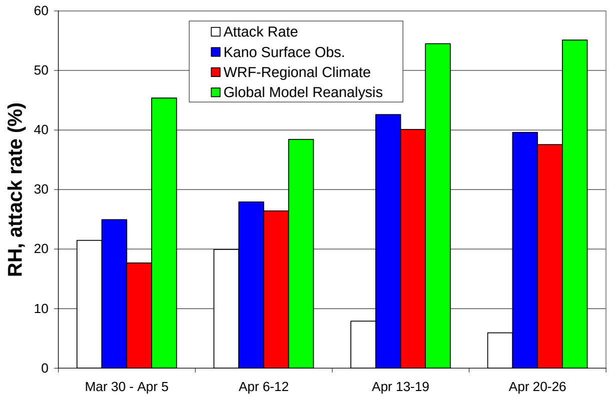


Figure 19. Comparison of meningitis attack rate (black-white) and relative humidity (%); observed in blue, WRF simulation in red and NCEP/NCAR reanalysis in green.

**Acknowledgements**

NCAR is sponsored by the National Science Foundation.

## REFERENCES

Adedokun, J. A. 1978: West African Precipitation and Dominant Atmospheric Mechanisms. *Arch. Met. Geoph. Biokl.,* Ser. A, 27, 289-310.

Afiesimama, E. A., 2007: Annual cycle of the mid-tropospheric easterly jet over West Africa. *Theoretical and Applied Climatology*, 90, 103-111.

Ati, O. F., C. J. Stigter, and E. O. Oladipo, 2002: A comparison of methods to determine the onset of the growing season in northern Nigeria*. Int. J. Climato*l., 22, 731–742.

Aumann, H.H., Chahine, M.T., C. Gautier, M.D. Goldberg, E. Kalnay, L.M. McMillan, H. Revercomb, P.W. Rosenkranz, W.L. Smith, D.H. Staelin, L.L. Strow, and J. Susskind, 2003: AIRS/AMSU/HSB on the Aqua Mission: Design, Science Objectives, Data Products, and Processing Systems. *IEEE Transactions on Geoscience and Remote Sensing*, 41, 253-264.

Besancenot, J.P., M. Boko, P.C. Oke, 1997: Weather conditions and cerebrospinal meningitis in Benin (Gulf of Guinea, West Africa). *European Journal of Epidemiology,* 13, 807–815.

Diedhiou A, Janicot S, Viltard A, de F´elice P, Laurent H., 1999: Easterly wave regimes and associated convection over West Africa and the tropical Atlantic: Results from the NCEP/NCAR and ECMWF reanalyses. *Clim. Dyn*. 15, 795–822.

Drobinski, P., S. Bastin, S. Janicot, O. Bock, A. Dabas, P. Delville, O. Reitebuch, and B. Sultan, 2009: On the late northward propagation of the West African summer monsoon in summer 2006 in the region of Niger/Mali. *J. Geophys. Res*., 114, D09108, doi.10.1029/2008JD0011159.

Eldridge, R. H., 1957: A synoptic study of West African Disturbance Lines. *Q. J. Roy. Meteorol. Soc.*, 83, 303–314.

Eltahir, E. A. B., Gong, 1996: Dynamics of wet and dry years in the West Africa. .*J.Clim*. 9, 1030-1042

Flaounas, E., S. Bastin, S. Janicot, 2010: Regional climate modelling of the 2006 West African monsoon: sensitivity to convection and planetary boundary layer parameterisation using WRF. *Clim Dyn*. 1432-0894.

Greenwood B. 1979: Manson lecture. Meningococcal meningitis in Africa. *Transactions of the Royal Society of Tropical Medicine and Hygiene,* 93, 341–53.

Gu G., R.F. Adler. 2004. Seasonal evolution and variability associated with the West African monsoon system. *J Clim,* 17, 3364–3377

Hagos, S. M., and K. H. Cook, 2007: Dynamics of the West African monsoon jump. *J. Climate*, 20, 5264–5284.

Hagos, and K. Cook, 2009: Development of a Coupled Regional Model and Its Application to the Study of Interactions between the West African Monsoon and the Eastern Tropical Atlantic Ocean*. J. Clim,* 22, 2591-2604.

Hamilton, R. A., and J. W. Archbold, 1954: Meteorology of Nigeria and adjacent territory. *Q. J. Roy. Meteol. Soc.,* 71, 231-264.

Hare, F. K., 1977: Takoradi-Khartoum air route: General synoptic climate. *Climatic Change*, 1, 157-172.

Janicot. S. and Co-authors, 2008: Large-scale overview of the summer monsoon over West Africa during the AMMA field experiment in 2006. *Annales Geophysicae,* 26(9), 2569-2595.

Kalnay, E., and Coauthors, 1996: The NCEP/NCAR 40-Year Reanalysis Project. *Bull. Amer. Meteor. Soc*., 77, 437–471.

Kiladis, G. N., C. D. Thorncroft, and N. M. J. Hall, 2006: Three-Dimensional Sturcture and Dynamics of African Easterly Waves. Part I:Observations*, J. Atmos. Sci.*, 63, 2212-2230.

Kiladis, G. N., M. C. Wheeler, P. T. Haertel, and P. E. Roundy, 2009: Convectively coupled equatorial waves, *Rev. Geophys*. 47, RG2003, doi:10.1029/2008RG000266

Knippertz and A. H. Fink, 2008: Dry-season precipitation in tropical West Africa and its relation to forcing from the extratropics. *Mon. Wea. Rev*., 136 (9), 3579–3596.

Knippertz and A. H. Fink, 2009: Prediction of Dry-Season Precipitation in Tropical West Africa and its Relation to Forcing from the Extratropics. *Weather and Forecasting*. doi: 10.1175/2009WAF2222221.1

Kuettner, J. P., and D. E. Parker, 1976: GATE: report of the field phase. *Bull. Amer. Met. Soc*., 57, 11-27.

Lélé, M. .I., and P. J. .Lamb, 2010. Variability of InterTropical Front (ITF) and Rainfall over West African Soudano-Sahel. *J. Clim*.. In press.

Liebmann B. and C.A. Smith, 1996: Description of a Complete (Interpolated) Outgoing Longwave Radiation Dataset. *Bulletin of the American Meteorological Society*, 77, 1275-1277.

Mekonnen, A., C. D. Thorncroft, A. R. Aiyyer, and G. N. Kiladis, 2008: Convectively coupled Kelvin waves over tropical Africa during the boreal summer: Structure and variability, *J. Clim*., 21, 6649–6667.

Molesworth, A. M., 2003: Environmental risk and meningitis epidemics in Africa. *Research Emerging Infectious Diseases*, 9, 1287-1293.

Multi Disease Surveillance Center, 2009: Weekly feedback bulletin on cerebrospinal meningitis, Week 17, 2009. 01 BP 549 Ouagadougou 01, Burkina Faso, http://www.meningvax.org/press-reports.htm

Nguyen, H. and J. P. Duvel, 2008: Synoptic wave perturbations and convective systems over equatorial Africa. *J. Clim*., 21, 6372–6388.

Omotosho, B. , A..A. Balogun, K. Ogunjobi. 2002: Predicting monthly and seasonal rainfall, onset and cessation of the rainy season in West Africa using only surface data. *Int. J. Climatol*. 20, 865–880.

Parker, D.J., R. R. Burton, A. Diongue-Niang, R. J. Ellis, M. Felton, C. M. Taylor, C. D. Thorncroft, P. Bessemoulin and A. M. Tompkin, 2005: The diurnal cycle of the West African monsoon circulation. *Quart. J. Roy. Meteor. Soc.,* 131, 2839–2860.

Parker D.J, Fink A, Janicot S, Ngamini J-B, Douglas M, Afiesimama E, Agusti-Panareda A, Beljaars A, Dide F, Diedhiou A, Lebel T, Polcher J, Redelsperger J-L, Thorncroft CD, Wilson GA. 2008: The AMMA radiosonde program and its implications for the future ofatmospheric monitoring over Africa. *Bull. Am. Meteorol. Soc*. 89, 1015–1027.

Pospichal, B., D.B. Karam, S. Crewell, C. Flamant, A. Hunerbein, O. Bock and F. Saıd. 2009: Diurnal cycle of the intertropical discontinuity over West Africa analysed by remote sensing and mesoscale modeling. *Quarterly Journal of the Royal Meteorological Society*, DOI: 10.1002/qj.435

Ramel R, Gall´ee H, Messager C. 2006: On the northward shift of the West African monsoon. Clim. Dyn. 26(4), 429–440.

Redelsperger J-L et al., 2002: Multi-scale description of a sahelian synoptic weather system representative of the West African monsoon. *Q J R Meteorol Soc* 128:1229–1257

Reed, R. J., D. C. Norquist, and E. E. Recker, 1977: The structure and properties of African wave disturbances as observed during phase III of GATE, *Mon. Weather Rev*., 105, 317–333.

Roundy, P.E. and W. M. Frank, 2004: A climatology of waves in equatorial region. *J. Atmos. Sci*., 61, 2105–2132.

Sijikumar S, Roucou P, Fontaine B. 2006: Monsoon onset over Sudan-Sahel: Simulation by the regional scale model MM5. *Geophys. Res. Lett*., 33, L03814. doi:10.1029/2005GL024819.

Skamarock, W. C., J. B. Klemp, J. Dudhia, D. O. Gill, D. M. Barker, M. Duda, X.-Y. Huang, W. Wang and J. G. Powers, 2008: A Description of the Advanced Research WRF Version 3. *NCAR Technical Note,.*

Straub, K. H., and G. N. Kiladis, 2002: Observations of a convectively coupled Kelvin wave in the eastern Pacific ITCZ. *J. Atmos. Sci*., 59, 30–53

Straub, K. H., and G. N. Kiladis, 2003a: Extratropical forcing of convectively coupled Kelvin waves during austral summer. *J. Atmos. Sci*., 60, 526–543.

Straub, K. H., and G. N. Kiladis, 2003b: Interaction between the boreal summer intraseasonal oscillation and higher-frequency tropical wave activity. *Mon. Wea. Rev*., 131, 945–960.

Sultan B, Janicot S. 2003. The West African monsoon dynamics. Part II: The “Preonset” and “Onset” of the summer monsoon. *J. Climate.* 16, 3407–3427.

Sultan B, Labadi K, Guegan JF and Janicot S, 2005: Climate drives the meningitis epidemics onset in west Africa. *PLoS Med*, 2, e6.

Thomson, M. C., A. M. Molesworth, M. H. Djingarey, K. R. Yameogo, F. Belanger, and L. E. Cuevas, 2006: Potential of environmental models to predict meningitis epidemics in Africa. *Trop. Med. and Int. Health*, 11, 781-788.

Vizy, E. K, and K. H. Cook, 2001: Mechanisms by which Gulf of Guinea and Eastern North Atlantic Sea Surface Temperature anomalies can influence African rainfall*. J. Climate*, 14, 795-821.

Wang, H., and R. Fu, 2007: The influence of Amazon rainfall on the Atlantic ITCZ through convectively coupled Kelvin waves. *J. Climate*, 20, 1188–1201.

Wheeler, M., G. N. Kiladis, 1999: Convectively coupled equatorial waves: Analysis of clouds and temperature in the wavenumber–frequency domain. *J. Atmos. Sci*., 56, 374–399.

Wheeler, M., G. N. Kiladis, and P. J. Webster, 2000: Large-scale dynamical fields associated with convectively coupled equatorial waves. *J. Atmos. Sci*., 57, 613–640.

Wolff, D.B and B.L. Fisher. 2008: Comparisons of Instantaneous TRMM Ground Validation and Satellite Rain-Rate Estimates at Different Spatial Scales. *Journal of Applied Meteorology and Climatology* 47(8), 2215-2237.

Xie, S-P., J.A. Carton, 2004: Tropical Atlantic Variability: Patterns, Mechanisms, and Impacts. In: in Earth Climate: The Ocean-Atmosphere Interaction,. C. Wang, S.-P. Xie, and J. A. Carton (eds.), Geophysical Monograph, AGU, Washington, D.C..

Yaka, P., B. Sultan, H. Broutin, S. Janicot, S. Philippon, N. Fourquet. 2008: Relationships between climate and year-to-year variability in meningitis outbreaks: a case study in Burkina

Faso and Niger. *International Journal of Health Geographics*, 7, 34.
Zhang, X. 2007: Adapting the Weather Research and Forecasting Model for the Simulation of Regional Climate in East Africa. Ph.D. Thesis. North Carolina State University.